AN INVESTIGATION OF COSINE ERROR FOR SCANNING PROBE MEASUREMENTS OF FREEFORM SURFACES

ChaBum Lee[1], Joshua Tarbutton[2], and Tony L. Schmitz[2]
[1]Department of Mechanical Engineering
Texas A&M University, College Station, TX
[2]Department of Mechanical Engineering and Engineering Science
University of North Carolina at Charlotte, Charlotte, NC

INTRODUCTION

Freeform optics represent geometries that are, in general, neither planar nor spherical and remove the traditional requirement of rotational symmetry from optical designs. Freeform surfaces introduce radical new design freedom into optical assemblies. However, they also generate inherent manufacturing and measurement challenges. For example, the traditional Fizeau interferometer that relies on planar and spherical reference wavefronts to compare against the surface under test is not well suited to freeforms with significant departures from these traditional geometries.

Surface measurement by point probe scanning instruments, whether the instrument transduction scheme is mechanical or optical, is ultimately a convolution of the measuring machine error motions, the point probe geometry (e.g., roundness of a nominally spherical tip), and the desired surface under test. While these are critical considerations that have been extensively explored in the literature, in this paper, the specific measurement issue to be examined is the cosine error that is introduced by a non-normal direction of the (linear) probe axis with respect to the surface under test.

This study introduces a novel methodology for the machined optical surface metrology that integrates a displacement probe in a precision spindle. To eliminate cosine error, the displacement probe is always placed normal to the measurement target surface by rotating the probe. Spindle rotational error measured by a reversal method [1-3] was compensated for in the surface profile measurement. The optical concave and convex mirror surfaces and bearing bore and outer surfaces are measured by the proposed method, and the uncertainty sources associated with the proposed measurement method are discussed. The paper is organized as follows. First, the cosine error is defined. Second, a measurement strategy is presented to highlight cosine error for a simple artifact geometry. Third, an experimental validation of the proposed measurement method is presented with artifacts. Fourth, conclusions are presented.

COSINE ERROR

Cosine error is a well understood phenomenon in displacement measurement. In a displacement measuring interferometry (DMI), for example, the DMI axis is not, in general, exactly aligned with the motion axis direction; see Fig. 1. The misalignment angle, θ, represents a cone of possible angular misalignments. This introduces uncertainty into the displacement measurement, but perhaps more importantly, it also results in a measurement bias. Regardless of the θ value, the measured displacement is always less than the (unknown) actual displacement. Cosine error can be modeled as shown in Eq. 1, where d_m is the measured displacement and d is the actual displacement.

$$d_m = d\cos\theta \tag{1}$$

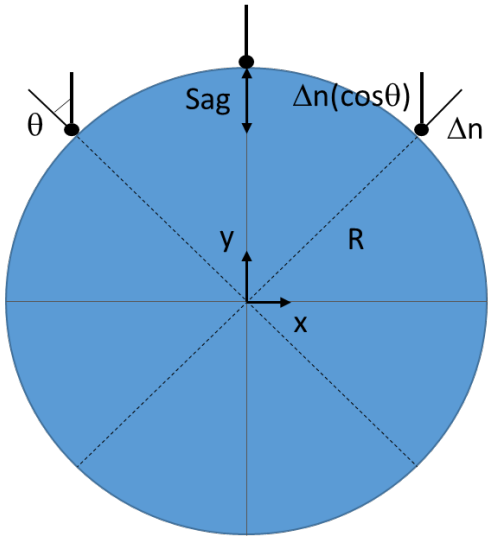

Figure 1. Cylinder measurement using a probe axis oriented in the y direction.

Cosine error also exists for point probe scanning measurements of non-planar, including freeform, surfaces. The situation is described by the surface measurement of a cylinder shown in Fig. 1. Here, the linear probe axis direction is fixed in the *y* direction. As the probe scans the surface, the angle between

the probe (measurement) axis and the surface normal varies. The angle, θ, is large at the extreme x locations (left and right) and zero in the middle at the cylinder apex. The angle value is $\sin\theta = x/R$, where R is the cylinder radius. Consider a Δn "bump" on the surface at any circumferential location. The deviation measured by the linear probe, Δy, depends on θ and is always less than the actual deviation (except at the apex). See Eq. 2.

$$\Delta y = \Delta n \cos\theta \qquad (2)$$

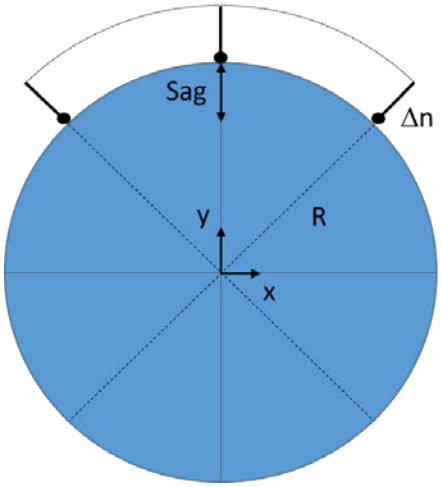

Figure 2. Cylinder measurement using a probe axis oriented in the surface normal direction.

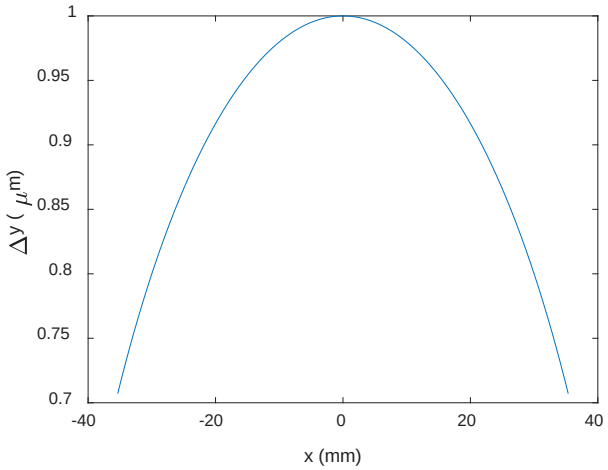

Figure 3. Probe "bump" height as a function of the scanning position, x, for the Fig. 1 orientation.

To eliminate this cosine error and corresponding bias, the linear probe direction can be maintained along the surface normal. This requires rotation about the z axis (i.e., the C rotary axis) in addition to the x and y scanning motions. The new measurement path is depicted in Fig. 2. Here the probe's displacement axis is always normal to the cylinder's surface.

Consider an example of a 50 mm radius and a θ variation of -45 deg to +45 deg (left to right in Fig. 1, x = -35.355 mm to 35.355 mm). If the "bump" size is Δn = 1 μm, the corresponding probe value for the Fig. 1 y direction orientation is provided in Fig. 3. It is observed that that error varies from 29.3% to zero and back to 29.3%. If the Fig. 2 measurement path is selected, on the other hand, the cosine error contribution is eliminated. The sag for this example is $R - (R^2 - x^2)^{0.5}$ = 16.645 mm.

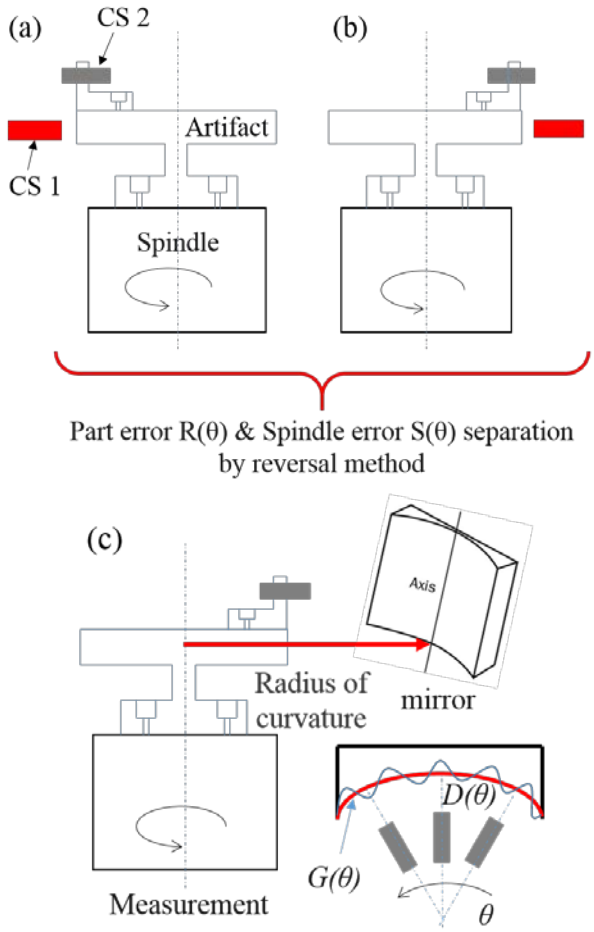

Figure 4. Reversal method: (a) measurement at θ = 0 deg, and (b) measurement at θ = 180 deg; (c) the proposed surface profile measurement method: angular displacement θ, part error R(θ), spindle error S(θ), sensor output D(θ), and surface profile G(θ).

MEASUREMENT METHOD

The proposed measurement system illustrated in Figure 4 consists of an aerostatic bearing spindle, two capacitive sensors (CS), a sensor holder, and an

artifact attached on the spindle shaft. Because the rotating accuracy of a spindle directly affects the CS 2 output, the spindle error S(θ) was separated from the part (artifact) error R(θ) by a reversal method proposed by Brian and Donaldson [4-5]. First, the artifact is positioned at an arbitrary angular position on the spindle, and a roundness trace is acquired from CS 1. Then, the CS 1 and the artifact are rotated by 180 deg. A new roundness trace is then acquired. Figure 4a and b show the two reversal positions. In position 1 (Figure 4(a)), the CS 1 reads a measured signal $m_1(\theta)$ given by:

$$m_1(\theta) = R(\theta)+S(\theta). \quad (3)$$

In position 2 (Figure 4b), the CS 1 reads a measured signal $m_2(\theta)$ given by

$$m_2(\theta) = R(\theta)-S(\theta). \quad (4)$$

Then, the part and spindle errors can easily be obtained as:

$$R(\theta) = (m_1(\theta)+m_2(\theta))/2, \quad (5a)$$

$$S(\theta) = (m_1(\theta)-m_2(\theta))/2. \quad (5b)$$

After separating spindle error from the part error, the measurement target (mirror surface with a radius of curvature, R_o) is placed with the offset distance from the spindle rotational axis that is the same as a radius of curvature of the measurement target and its surface profile can be obtained by rotating the spindle. This measurement enables the measurement probe to be always placed toward to the measurement target surface at a right angle. However, because this surface profile information includes spindle error, the corrected surface profile can be expressed as:

$$G(\theta) = R_o+\Delta D(\theta)-S(\theta),\ \Delta D(\theta)= D(\theta)- D_o, \quad (6)$$

where R_o is the radius of curvature of the measurement target and D_o is the initial offset distance of CS 2 at the beginning of the measurement. See Figure 4c.

SETUP AND MEASUREMENT RESULTS

The experimental setup is shown in Figure 5. The measurement was performed in a vibration-controlled lab environment. An aerostatic bearing spindle (Dover Instrument) and two identical capacitive sensors (Capacitec, 10 nm resolution, effective sensing diameter of 5 mm) are employed for the experiment. To eliminate the spindle dynamic effects and brushless DC motor effects, the measurement data was discretely collected from the equally spaced points of the target surface and was averaged. Surface profiles of the concave (R_o 95 mm) cylindrical lens were measured by the proposed measurement system.

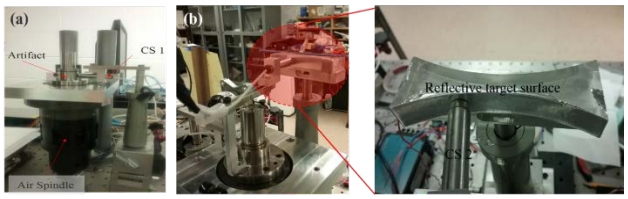

Figure 5. Experimental setup: (a) spindle and CS 1 only, and (b) full setup and detailed image.

The spindle error was separated by the reversal method; the results are shown in Figure 6. The spindle motion was measured in 10 deg intervals twice. From Equation 4, the spindle error S(θ) was 0.081 µm and its peak-to-valley (PV) value was 0.298 µm. Also, the part error R(θ) was 0.217 µm and its PV value was 0.786 µm.

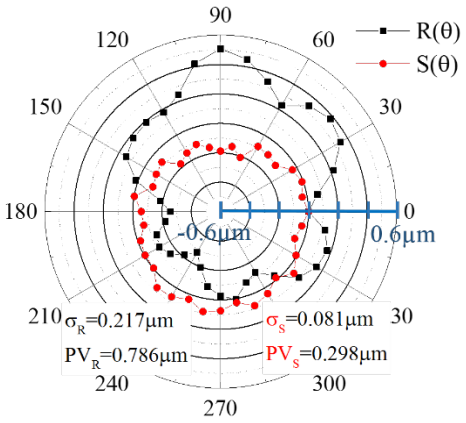

Figure 6. Results of spindle error separation.

As shown in Figure 4, after separating the spindle error from the part error, the displacement probe scans the cylindrical mirror and, then, the surface profile ΔG(θ) that subtracts R_0 from G(θ) can be calculated from Equation 5. The aluminum foil tapes were adhered to the acrylic cylindrical concave and convex lenses to make it conductive for capacitance measurement between the probe and target surfaces. Concave and convex target surfaces were placed 95 mm and 100 mm away from the center of the spindle rotational axis for each measurement, respectively. By rotating the spindle axis to always orient the measurement probe normal to the target surface, each target surface was measured three times with at equal intervals of 5 mm over 87 mm. From the results shown in Figure 7, the PV value for the concave surface profile was approximately 27 µm and the measurement standard deviation (from three measurement results) was 0.24 µm (Figure 7b).

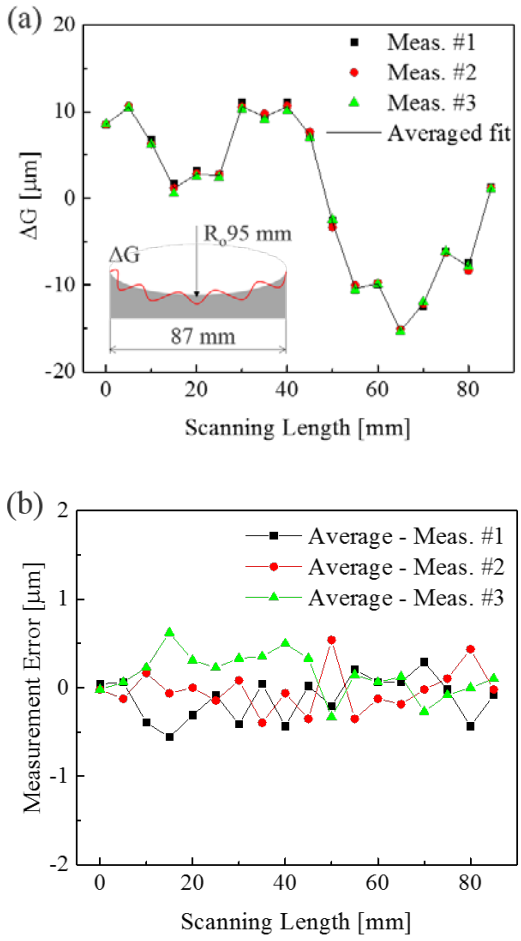

Figure 7. Surface profile measurement results of concave lens R_o 95 mm: (a) surface profile and (b) measurement deviation.

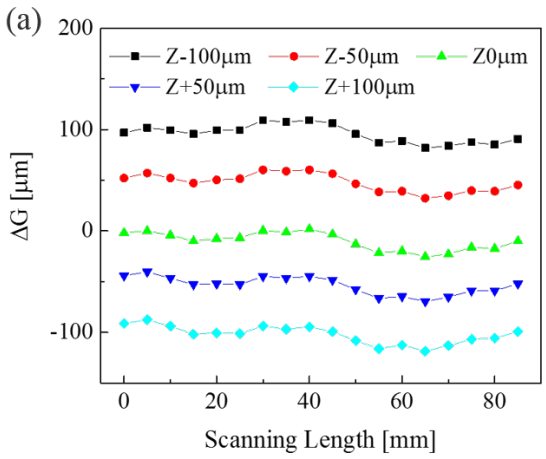

Figure 8. Measurement target surface positioning effects on surface profiles.

In the proposed measurement method, placing the target surface at the correct position (the same as the radius of curvature of each target) from the spindle rotation axis is critical to the surface profile measurement. Because there may exist spindle rotation axis-to-target surface positioning error, the effects of positioning error on surface profile measurement were investigated by measuring the surface profile at various positions along the Z-axis. The offset distance between spindle rotation axis and target surface varies from -100 μm to +100 μm (at a given distance R_o) and the manual linear stage with the micrometer was used to move the target surface forward and backward. The offset distance from -100 μm to +100 μm was selected because such positioning accuracy of the target surface can be easily achieved, even manually, in measurement alignment processes. Similarly to the previous measurements in Figure 7, each target surface was measured at equal intervals of 5 mm over 87 mm. Also, the measurement data was discretely collected from the equally spaced points of the target surface and was averaged to eliminate the spindle dynamic effects and brushless DC motor effects. From the result of Figure 8, at a given offset distance (±100 μm), the measured surface profiles showed trends over the offset distances for both concave and convex surfaces. These results indicate that the proposed measurement method is effective for measuring both the concave and convex surfaces and is not significantly sensitive to the offset distance between the spindle rotation axis and the measurement target surface.

As a part of measurement uncertainty estimation of the proposed system, the surface profile error could result from four alignment errors: (a) probe offset error, (b) probe angular alignment error, (c) probe distance error along the radial direction and (d) target positioning error. In this study, the probe with an effective sensing diameter of 5 mm was used, so the probe offset error and probe angular alignment error can be neglected. However, as the sensing area of the probes gets smaller, those errors could be significant to the surface profile measurement. The probe distance effect along the radial direction be neglected because the probe only picks up the constant gap distance between the probe and target surface. However, depending on the probe type, such as a laser-based displacement sensor, eddy current sensor, or LVDT (linear variable differential transformer), and its effective sensing area, this error can be significant. Measurement uncertainty of the proposed system depending on the probe type will be investigated in future work.

CONCLUSIONS

A measurement method that eliminates cosine error, particularly for optical surface metrology, was proposed. Cosine error can be eliminated through always aligning the probe normal to the target surface by rotating the probe attached on the spindle axis. Spindle rotation error was compensated in the surface profile data using a reversal method. The proof of the concept was tested and it was confirmed that the proposed measurement system can be applied for measuring both concave and convex surface profiles. As a result, the measurement method can both eliminate cosine error and scan the large area quickly. In addition, the proposed measurement system can be used for freeform surface measurement by integration with precision machine tools for on machine measurement applications.

ACKNOWLEDGEMENTS

The research was supported by the National Science Foundation (Award Number: CMMI 1663210) through Texas A&M University and (Award Number: CMMI 1663405) through University of North Carolina at Charlotte.

REFERENCES

1. Donaldson, R.R., A simple method for separating spindle error from test ball roundness error, Annals of the CIRP, 21, 125–126, (1972).
2. Eric R. Marsh, Precision Spindle Metrology, DEStech Publication Inc., 2010.
3. Bala Muralikrishnan and Jay Raja, Computational Surface and Roundness Metrology, (Springer, 2009).
4. Yadong Li, Peihua Gu, Free-form surface inspection technique state of the art review, Computer-Aided Design, 36(13), 1395-1417 (2004).
5. Jin-Ho Kang, ChaBum Lee, Jae-Young Joo, and Sun-Kyu Lee, Phase-locked loop based on machine surface topography measurement using lensed fibers, Applied Optics, 50(4), 460-467 (2011).